Gain-Scheduled FDI for a Re-entry Vehicle

Murray L. Kerr*, Andrés Marcos† and Luis F. Peñin‡
Deimos Space S.L., Madrid, 28760, Spain

and

Eric Bornschlegl§
European Space Agency (ESA) ESTEC, Noordwijk, 2200, The Netherlands

This paper presents the design of a gain scheduled fault detection and isolation (FDI) filter for the Hopper reusable launch vehicle (RLV). The fault scenario is that of faults in the vehicle's rudder actuator and sideslip sensor during a focused 90 second period of the re-entry. Both of the considered faults strongly affect the lateral response of the vehicle, making simultaneous FDI difficult. A dynamically stable model of the Hopper RLV is considered and FDI filter design is performed on linearised models of the vehicle trimmed about the re-entry trajectory. H-infinity theory is employed for the FDI filter synthesis, with a set of LTI FDI filters designed at the trim points and then scheduled to form the gain scheduled FDI filter. The effectiveness of the LTI point-design filters and the gain-scheduled filter are determined by simulation using a tightly gain-scheduled model of the linearised vehicle's open-loop response that captures the strongly parameter varying vehicle behaviour as it tracks the re-entry trajectory. The advantages of using gain-scheduled FDI filters for FDI on RLVs are highlighted via the simulations.

Nomenclature

Δ	= Norm bounded complex uncertainty
d	= Disturbance
f	= Generic fault
f_s	= Sensor fault
f_a	= Actuator fault
$\hat{f}$, res	= Fault estimate
$\hat{f}_s$, res_s	= Sensor fault estimate
$\hat{f}_a$, res_a	= Actuator fault estimate
F	= FDI filter
F_Y ,F_U, Q	= FDI filter subelements
$F_l(\cdot,\cdot)$	= Lower LFT interconnection
G	= Generic vehicle model
G_u	= Vehicle model element accepting plant input
G_d	= Vehicle model element accepting disturbance input
G_f	= Vehicle model element accepting fault input
K_a , K_s	= Fault location selectors
M	= LFT interconnection of P and F, $M = F_l(P,F)$
n	= Noise

* Senior Control Engineer, Deimos Space. murray.kerr@deimos-space.com.
† Senior Control Engineer, Deimos Space.
‡Project Manager and Head of the Simulation and Control section, Deimos Space. Senior AIAA member.
§ Technical Officer, ESA ESTEC.

p, q, r	= Body axis roll, pitch and yaw rate
P , $\overline{P}$	= Generic plant in LFT interconnection
u	= Plant input
R	= Vehicle geocentric altitude
Vt	= Vehicle speed
w_a	= Uncertainty input
y	= Plant output
z_a	= Uncertainty output

I. Introduction

Due to the high cost and risk of aerospace projects, there is an increasing requirement that vehicles be capable of monitoring and managing their own health in the event of subsystem failures. One way to provide such functionality is through on-line fault detection and subsequent vehicle reconfiguration capabilities, either at the hardware or the software level. This paper considers the problem of the design of fault detection and isolation (FDI) filters for a reusable launch vehicle (RLV) that would form part of the health monitoring capabilities of the vehicle. Specifically, FDI filters are designed for a model of the Hopper RLV during re-entry (see Ref.1 and the references therein for details on the Hopper RLV).

The design of FDI filters for re-entry vehicles was previously considered in the work of Ref.2. In Ref.2 LTI FDI filters were designed using H-infinity theory for reaction control system (RCS) failures during the early re-entry phase of the Shuttle vehicle. The effectiveness and robustness of the designed filters was evaluated based on LTI models of the vehicle (ie operating at frozen trimmed points in the trajectory). More recent work on the application of H-infinity designed FDI filters to re-entry vehicles can be found in Ref.3, which considered the Shuttle vehicle operating in the transonic region near the end of the re-entry trajectory. In Ref.3 actuator failures were considered, with the effectiveness and robustness of the designed filters again evaluated based on LTI models of the vehicle.

In contrast to previous works on FDI of re-entry vehicles, in this paper both LTI and gain-scheduled (GS) FDI filters are designed. The FDI filters are designed using H-infinity theory, with LTI FDI filters designed for the trimmed vehicle at specific trim points, termed point-design filters. Based on these point-design filters, a GS FDI filter is then designed using a quadratic scheduling law. To highlight the advantages of gain scheduling the FDI filters, and also in contrast to previous works, the FDI capabilities of the filters are evaluated on a tightly gain scheduled model of the linearised vehicle's open-loop response that captures the strongly parameter varying nature of the vehicle dynamics while tracking the re-entry trajectory. This evaluation on the gain scheduled vehicle model is important, as it captures one of the main difficulties in FDI for re-entry vehicles; that of the vehicle's dynamic behaviour being inherently parameter varying due to the evolution of the vehicles states as it tracks the re-entry trajectory. As shown in the paper, this feature of the re-entry problem leads naturally to the requirement that the FDI filter must be also parameter varying, which is here provided for via the scheduling of the designed LTI filters.

The paper is structured as follows. Section II presents the Hopper RLV FDI problem and fault scenario. Section III presents the modeling of the Hopper vehicle for FDI filter design. Section IV presents a review of model based H-infinity open-loop FDI design theory. Section V presents the design of the point-design FDI filters and of the gain-scheduled FDI filter. Section VI presents the evaluation of the designed filters on the frozen LTI plant models and also on the more realistic gain scheduled LTI model. Conclusions and future work are detailed in Section VII.

II. Problem Statement

The Hopper RLV was designed to perform sub-orbital point-to-point flights. In the present FDI scenario a focused time period within the *re-entry phase* for the Hopper is considered, with the vehicle controlled by an existing NDI controller[1] that ensures the vehicle tracks a predefined re-entry trajectory. The time period considered is from 1410 to 1500 seconds of the flight, which corresponds to a period near the end of the re-entry phase (see Figure II-1). This was chosen for the FDI design problem, as it corresponds to a period where full aerodynamic controls are employed and where the vehicle behaviour changes sufficiently to test the robustness properties of the designed filters.

Considering Figure II-1, it is seen that over this period the trimmed attitude angles are roughly constant (the main exception being a 2.5 degree variation in the angle of attack) but the translational variables change significantly, with the trimmed velocity, Mach and geocentric altitude changing by 390 m/s, 1.2 and 3.5 km, respectively. The

aero surface configuration is also dynamically changing, as opposed to the saturated configuration in the early re-entry time[1]. Hence the vehicle trim configuration is dynamically changing.

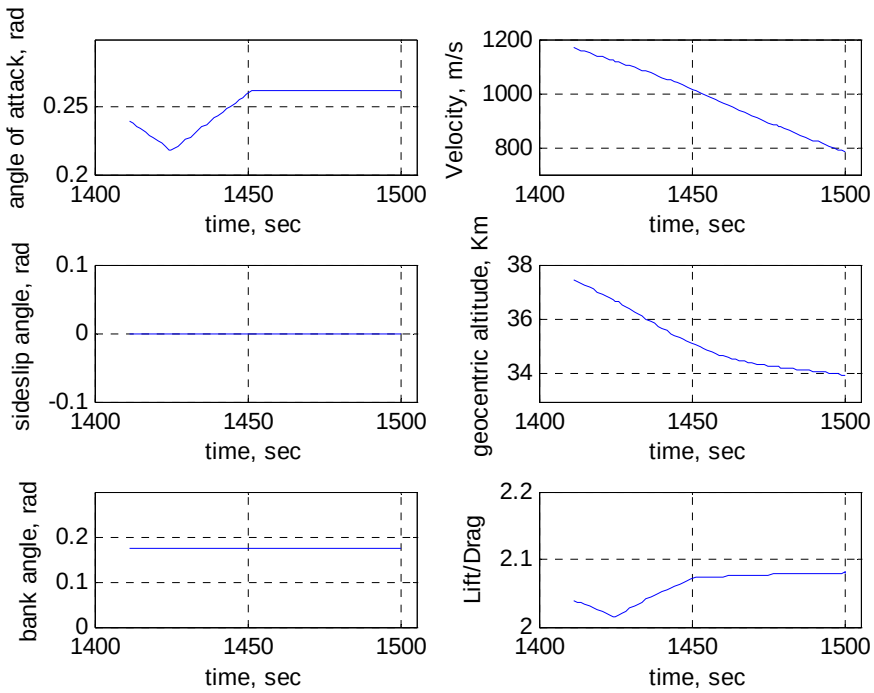

Figure II-1 Re-entry trajectory period considered in the fault scenario

A. Selected Fault Scenario

In the present work, the vehicle is assumed to be subject to actuator and sensor faults, being a fault in the rudder actuator and sideslip sensor. This actuator and sensor fault set was chosen due to the importance of faults in this actuator and sensor on the vehicle response[4] and because both faults strongly affect the vehicle lateral/directional motion, making the design problem more challenging; the rudder is the main lateral effector and sideslip the main lateral sensor (together with the yaw rate sensor). Subsequently, the FDI filter is to be designed to detect faults in either the rudder actuator or sideslip sensor. Here is it not assumed that these faults act in a mutually independent manner, and hence the FDI filter must be designed to simultaneously detect faults in each actuator and sensor and ensure such faults do not have a significant adverse effect on the fault detection capabilities in the other channel. Hence this specific choice of faults presents a challenging FDI problem and one that highlights the challenges associated with designing FDI filters for this type of vehicle.

B. FDI Design Problem

One feature of the present FDI problem is that the Hopper RLV is dynamically unstable over the considered period. This presents several potential problems for FDI filter design. Firstly, it is known that open-loop FDI on unstable vehicles is fundamentally difficult[5]. This suggests that an integrated FDI design approach should be employed[6] where the vehicle's controller and FDI filter are simultaneously designed. This is however not possible in the present scenario, as a controller already exists which cannot not be modified. A second plausible approach is to design FDI filters based on the system's closed-loop behaviour. This would however require linearisation of the closed-loop system due to the presence of the NDI controller, which itself is changing with the changing operating condition (ie body angle rates, velocity etc). Even if this were feasible, open-loop FDI is generally preferred to closed-loop FDI for the potential to reduce sensitivity to uncertainty[7] and is therefore the preferred choice for the FDI filtering approach on the Hopper RLV.

For the above reasons, as a first step in the solution of the *open-loop* FDI problem for the Hopper RLV, it was chosen to perform open-loop FDI on a modified model of the vehicle, where now the vehicle model is dynamically stable. This modification is detailed in Section III, where it is shown that the stable vehicle model's modal behaviour has a similar eigenstructure (eigenvectors and eigenfrequencies) to the unstable vehicle model, with the principal

alteration to the model being the mirroring of the unstable poles about the imaginary axis. Hence, while this modification represents a significant change in the FDI problem, the preservation of the vehicle's eigenstructure does ensure that the design problem is representative of that on a re-entry vehicle[**].

With this modification to the vehicle model made, the design problem is to synthesize open-loop FDI filters, based on stable open-loop models of the vehicle, for estimation of rudder actuator and beta sensor faults. As discussed in Section VI, a tightly scheduled model of the linearised and stable vehicle's open-loop response over the trajectory period will be used to assess the filter performance.[††]

III. Modelling for FDI Filter design

An important step in any model-based FDI design approach is that of obtaining a model of the nonlinear system that is suitable for FDI design. In the present work, the full 6DOF nonlinear model reported in Ref.1 forms the basis for the model development. For the scenario considered, representative models of the vehicle were developed by trimming and then linearising the nonlinear vehicle model about the selected part of the trajectory. This was performed at a number of trajectory points within the re-entry period considered using Matlab nonlinear optimization and linearisation routines. Specifically, the Hopper RLV was trimmed and linearised at 19 points on the nominal re-entry trajectory covering the re-entry period from 1410 to 1500 seconds (see Figure II-1), being the following re-entry times:

[1410, 1415, 1420, 1425, 1431, 1435, 1440, 1445, 1450, 1455, 1460, 1465, 1471, 1474, 1480, 1485, 1490, 1495, 1500]

This corresponds to the generation of locally valid LTI vehicle models every 5 seconds (approximately) within this trajectory period. This set of models was found to be sufficient to capture smoothly the variation in the vehicle behaviour over the trajectory period.

The resulting linearized models of the Hopper have 12 states, capturing both the attitude and translational dynamics (These LTI models do not include actuator or sensor dynamics). This 12 state model can be reduced to 6 states by considering only the lateral/directional dynamics of the vehicle: roll rate *p*, yaw rate *r*, sideslip angle *beta*, bank angle *sigma*, true airspeed *Vt*, and geocentric altitude *R*. This reduced order model was deemed sufficient for FDI purposes on the lateral/directional motion of the vehicle, which is the current FDI problem given the choice of actuator and sensor failure, since the linearised models displayed strong decoupling of the lateral/directional and longitudinal dynamics. The outputs of the vehicle model are its states. Therefore, each LTI plant consists of, ordered as given, six states (sideslip beta, yaw rate r, bank angle sigma, roll rate p, velocity Vt and geocentric altitude R), six outputs (sideslip beta, yaw rate r, bank angle sigma, roll rate p, velocity Vt and geocentric altitude R) and five inputs (outboard right elevon ERO, outboard left elevon ELO, inboard right elevon ERI, inboard left elevon ELI and rudder RUD). Note that the vehicles flaps are removed as an input, as they are only used for trimming purposes.

To highlight the properties of these reduced order vehicle models, a modal analysis of the trim point LTI model P_1471, corresponding to the re-entry trim point at the trajectory time of 1471 seconds, is given in Table III-1, along with the associated eigenvectors from the A matrix. The table also indicates the likely lateral mode that the eigenvector corresponds to (this is only an approximate match to standard aircraft modes). This matching is based on the fact that the Dutch roll mode is typically complex, the fastest and involves both axes; the spiral is the slowest and doesn't couple into beta; and, the roll mode couples both roll angle and rate response and is reasonably fast.

Considering the modal response of the Hopper, it is clear that the system is dominantly unstable, in that the spiral mode is unstable and also the faster Dutch roll mode. While the spiral mode could be neglected in a further reduced order model, the Dutch roll mode cannot. Hence when designing an FDI filter for the Hopper, the unstable dynamics corresponding to the Dutch roll mode would have to be accounted for in the design.

[**] Recall that the well-known space-shuttle re-entry example in Ref. 9, for which FDI filters were designed in Ref.3, is a stable system.

[††] While the evaluation is herein limited to LTI models of the vehicle, comparison with the full nonlinear model of the vehicle shows that the employed LTI models do give an accurate representation of the vehicle response for the range of control signals typically applied to the vehicle. Evaluation on the full nonlinear model requires closed-loop evaluation of the FDI filters, which is the subject of extensions to the present work (see Section VII).

As discussed in Section II, the approach taken in this work is to consider a stable model of this vehicle as a first step in the solution of the open-loop FDI problem on the unstable vehicle. The construction of this model is detailed in the proceeding section.

Table III-1: Modal analysis of the lateral Hopper dynamics at trajectory time 1471 (P_1471)

Poles	0.081 + 0.459 i 0.081 - 0.459 i		-0.180	7.259 e-5	-0.0036 + 0.0017 i -0.0036 - 0.0017 i	
States of A	{beta, r, sigma, p, Vt, R}					
Evectors (abs value)	0.0537	0.0537	0.0087	0.0000	0.0000	0.0000
	0.0890	0.0890	0.0377	0.0102	0.0000	0.0000
	0.9017	0.9017	0.9835	0.9999	0.0000	0.0000
	0.4113	0.4113	0.1731	0.0024	0.0000	0.0000
	0.0834	0.0834	0.0366	0.0000	0.1778	0.1778
	0.0039	0.0039	0.0045	0.0001	0.9841	0.9841
Mode	Dutch roll		Roll	Spiral	-	

1. Construction of a Stable Vehicle Model

Here the unstable dynamic modes of the vehicle model are stabilized by replacing the unstable poles with stable poles of the same frequency but with negative real rather than positive real part (ie $p_u = x + iy$ replaced with $p_s = -x + iy$). This was performed in a way that the vehicle's eigenstructure (eigenvectors and eigenfrequencies) were preserved, while clearly affecting the stability and hence the phase of the vehicle's frequency response.

A modal analysis on the now stable model of the lateral dynamics of the Hopper is shown in Table III-2 (The now stable spiral and Dutch roll modes are highlighted in bold). It is evident from a comparison with Table III-1 that the eigenvectors have now changed slightly (typically by less than 2% and sometimes negligibly). The main changes are naturally seen in the Dutch roll mode and to a lesser extent the spiral mode, with the spiral and roll mode eigenvectors essentially unchanged, and also those for the *Vt* and *R* response. Note that the now stable modes are at approximately the same frequency as the unstable modes, with the main difference being the now negative real part of the pole. Hence the modifications to the model have effectively replaced the unstable modes with stable modes, but importantly, this has been done in a way that preserves the eigenstructure of the vehicle. Therefore, the resulting model preserves many of the dynamical features of the vehicle, while providing a stable model for open-loop FDI design and open-loop FDI performance assessment.

Table III-2: Modal analysis of the **stable** *lateral Hopper dynamics after Dull roll mode factorisation and perturbation of the spiral mode*

Poles	**-0.081 + 0.459 i** **-0.081 - 0.459 i**		-0.180	**-2.071 e-5**	-0.0036 + 0.0017 i -0.0036 - 0.0017 i	
States of A	{beta, r, sigma, p, Vt, R}					
Evectors (abs value)	0.0522	0.0522	0.0087	0.0000	0.0000	0.0000
	0.0863	0.0863	0.0377	0.0102	0.0000	0.0000
	0.9018	0.9018	0.9835	0.9999	0.0000	0.0000
	0.4122	0.4122	0.1730	0.0025	0.0000	0.0000
	0.0813	0.0813	0.0366	0.0000	0.1778	0.1778
	0.0038	0.0038	0.0045	0.0001	0.9841	0.9841
Mode	Dutch roll		Roll	Spiral	-	

IV. Model-based H-infinity Open-loop FDI Design Theory

The FDI filters for the Hopper RLV are to be designed using model based H-infinity *open-loop* FDI design theory[6,8]. The essence of the model-based open-loop FDI problem is depicted in Figure IV-1. The problem to be solved is, given a model of the nominal system G_u, and knowledge (measured or estimated) of the inputs u and outputs y of the system, provided an estimate[‡‡] $res = \hat{f}$ of the faults f entering the system through the subsystem fault dynamics G_f. This estimate is generated by the FDI filter $F=[F_U\ F_Y]^T$ and can provide an indication of the fault's presence – *fault detection* – or also provide an indication of the fault location/source – *fault isolation*[6]. Hence fault detection requires only a single (scalar) fault estimate, while fault isolation requires a set (vector) of fault estimates in order to be able to distinguish between faults.

Most model based FDI approaches operate on the open-loop system and therefore use the inputs and outputs of this system for fault estimation. However, it is also possible to perform FDI based on knowledge of the inputs and outputs of the closed-loop system, comprised of the feedback connection of the open-loop system and a controller. There are significant differences between the properties of the two approaches[7], with open-loop FDI often being favored due to the potential for reduced sensitivity of the fault estimate to model uncertainty and its ability to retrofit the designed FDI filter on *any* existing controlled system. For both approaches, the requirements on the filter are the same:

i. To reliably and accurately detect and isolate faults.
ii. To be insensitive to exogenous disturbances, noise and system uncertainty.

These objectives lead to the natural requirement that the residual generator be robust, which is the main motivation for the employment of H-infinity optimization approaches, since one of their distinguishing features is that they are developed to explicitly account for system uncertainty in the solution of the optimization problem. As such, they provide for a direct way to trade-off the level of robustness to uncertainty with the level of performance of the FDI filter. This is especially important in filtering problems, due to their explicit open-loop nature, which makes the provided filtering properties sensitive to uncertainty. In the following subsections, the basic concepts for model-based open-loop FDI design, and specifically the H-infinity based solutions, are presented.

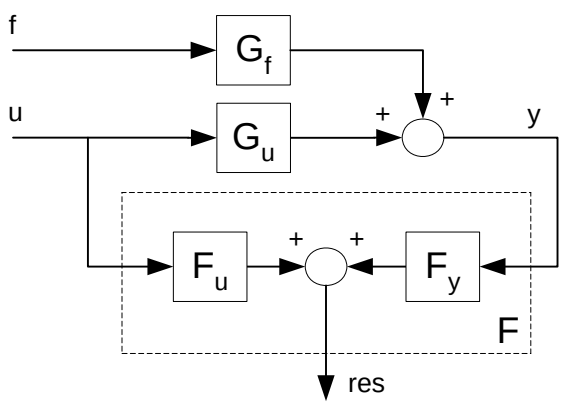

Figure IV-1 Basic FDI design architecture

C. Robust open-loop FDI filter design

The problem of designing a robust H-infinity FDI filter is generally divided in two main stages: first, robust residual generation and second, robust residual evaluation. We will focus on the first task, being the design a robust residual generator using H-infinity optimization techniques (the concepts presented in the next sub-section are quite generic and applicable to the general open-loop FDI problem). From the H-infinity perspective, the residual generation design problem can be divided in two parts:

---

‡‡ What is herein termed a "fault estimate" is often also referred to as a "residual signal" in the general FDI community. We prefer to use the former term to distinguish it from the general concept of a residual, which is any signal formed by subtracting from a measured signal its ideal version so that all effects not accounted for in the idealized signal (i.e. uncertainty, faults, noise, etc) are left in the residual version.

a) Transforming the problem into the standard H-infinity formulation.
b) Defining an appropriate optimization index.

2. Transformation to an H-infinity problem formulation

For simplicity in the presentation of the transformation, it is assumed that a generalized plant is available (actuators, sensors, and weighting functions are embedded in the plant description). Although this assumption does not affect the theoretical developments presented here, it is important in practice, since correct weight selection is necessary for the problem solution to be meaningful.

Assume the nominal system (i.e. with no model uncertainty) is given by:

$$y(s) = G_u(s)u(s) + G_d(s)d(s) + G_f(s)f(s) \tag{1}$$

The transfer function $G_u(s)$ determines the effects on the system of the known inputs $u(s) \in \Re^{nu}$; $G_f(s)$ determines the effects of the faults $f(s) \in \Re^{nf}$; and $G_d(s)$ determines the effects of the disturbances $d(s) \in \Re^{nd}$. These transfer functions are assumed to be known (ie LTI models of these transfer functions are available).

A generic residual generator with transfer function F is given by (see Figure IV-2):

$$res(s) = F(s)\begin{bmatrix} u \\ y \end{bmatrix} = Q(s)\left[-H_u(s)u(s) + H_y(s)y(s)\right] = Q(s)\left[G_f(s)f(s) + G_d(s)d(s)\right] \tag{2}$$

where $H_u(s)$, $H_y(s)$ and $Q(s)$ are sub-elements of the FDI filter F. Note that in Eq. 2 $H_u(s)$ and $H_y(s)$ have been substituted with their optimal values for rejection of the coupling of the control signal u on the fault estimate. Considering Eq. (2), it is evident that for good FDI the filter F needs to cancel or minimize the effect of the disturbances d while maximizing the effect of the faults f on the residual. This multi-objective optimization is not easily amenable for H_∞ techniques due to its min-max characteristics. Figure IV-2 shows the formulation of the plant from Eq. (1) and the filter from Eq. (2) (this is a more detailed version of the formulation in Figure IV-1).

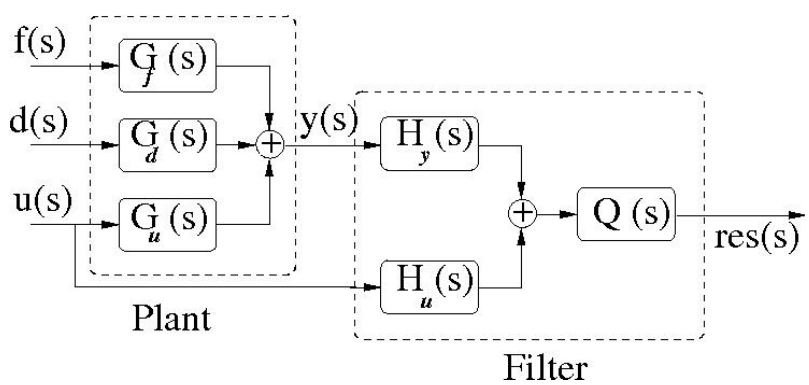

Figure IV-2 H_∞ nominal problem formulation

Using a state-space representation of the input/output systems from Eq. (1) and Eq. (2), together with the diagram from Figure IV-2, it is straightforward to transform the problem into the standard formulation (ie a linear fractional transformation (LFT)[9,10]) by "pulling-out" the FDI filter F (formed in this case by H_y, H_u and Q) as in Figure IV-3.

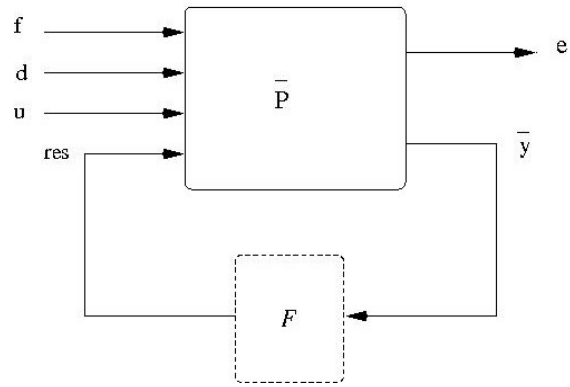

Figure IV-3 Standard nominal H_∞ filter problem

The output channel *e* represents the fault estimate error, the input *res* the diagnostic (fault estimate) signal, and the exogenous input channels can all be viewed as a generalized input vector comprised of disturbances *d*, faults *f*, and input command *u* vectors. Based on this standard problem formulation the *fault detection and isolation problem* is defined as the problem of finding a filter *F*, with input $\bar{y} = \begin{bmatrix} u^T & y^T \end{bmatrix}^T$, such that the fault performance error is minimized for all exogenous inputs.

Unfortunately, any mathematical system model is inaccurate and therefore has associated with it a level of uncertainty. This can be due to modelling errors and simplifications, parameters that vary during operation or unknown dynamics/parameters, among other uncertainty sources. Hence it is important to directly account for uncertainty in order to properly design a robust fault detection and isolation filter. From robust control theory the concept of uncertainty balls[8,9] can be used to define model uncertainty: $B_\Delta := \{\Delta(s) \in \Re H_\infty \,/\, \|\Delta\|_\infty < \gamma\}$, where γ defines the level of uncertainty. There are different uncertainty models, but the most common are multiplicative uncertainty and additive uncertainty models.

In Ref.6 a general residual generator is obtained under the assumption that all the system transfer functions have multiplicative uncertainty. The input-output representation of such a system is given by:

$$\begin{aligned} y &= G_u(I+\Delta_u)u + G_d(I+\Delta_d)d + G_f(I+\Delta_f)f = \\ &= G_u u + G_d d + G_f f + G_u\Delta_u u + G_d\Delta_d d + G_f\Delta_f f \end{aligned} \tag{3}$$

This multiplicative uncertainty form can also be represented by additive uncertainty models:

$$y = G_u u + G_d d + G_f f + \bar{\Delta}_u u + \bar{\Delta}_d d + \bar{\Delta}_f f \tag{4}$$

Figure IV-4 shows the standard nominal H-infinity filter problem from Figure IV-3 using a structured uncertainty operator, obtained from either a multiplicative (Eq. (3)) or an additive (Eq. (4)) uncertainty model representation. This formulation can be obtained by isolating the uncertainty terms $\tilde{\Delta}_\bullet$ in the system interconnection, which is a standard LFT construction procedure[9,10]. The resulting formulation is then in the desired $M-\Delta$ LFT representation for robust control, with $M = F_l(P,F)$ and $\bar{P}$ the generalized plant that captures all the known information about the nominal system *G* and its interconnection with the uncertainty terms $\tilde{\Delta}_\bullet$ and the FDI filter F.

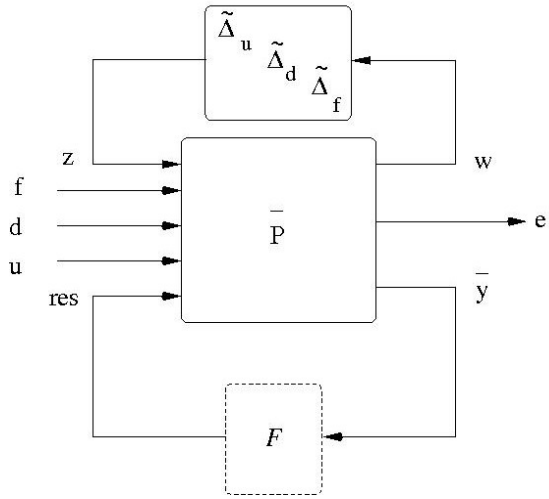

Figure IV-4 Standard H_∞ robust fault diagnosis problem.

3. Optimization indexes

Once the formulation of the problem has been posed in the standard robust set-up in Figure IV-4, an appropriate optimization index must be selected. The general objective of the robust H_∞ filter synthesis is to find a stable filter that maximizes the faults effect on the fault estimate, i.e. $max||TF_{f\to res}||_\infty$, while minimizing the effects of the remaining exogenous signals on the fault estimate, i.e $min||TF_{\nu\to res}||_\infty$ (where ν represents the aggregation of all the remaining exogenous inputs). These two objectives are not only opposing in some cases, but are also difficult to formulate simultaneously in the H_∞ optimization framework.

To overcome this problem, a model-matching technique is typically used to obtain an optimization index that satisfies the objectives[6]. The model-matching approach is based on the use of an ideal reference model (in this case for faults) Tf_{id}, which is typically diagonal for fault de-coupling purposes (isolability), and depending on the type of application it can be an identity matrix or a frequency dependent weight to emphasize the frequency band of interest. This ideal model also allows for a better blending of the optimization objectives (overcoming the min-max issue) by transforming the objective of maximizing the effect of the faults on the fault estimate into that of minimizing the error between the fault estimate and the weighted fault, i.e $max||TF_{f\to res}||_\infty \approx min||G_{f\to e}||_\infty \equiv min||\ res\text{-}\ Tf_{id} f\ ||_\infty$. Figure IV-5 shows this ideal fault model-matching problem.

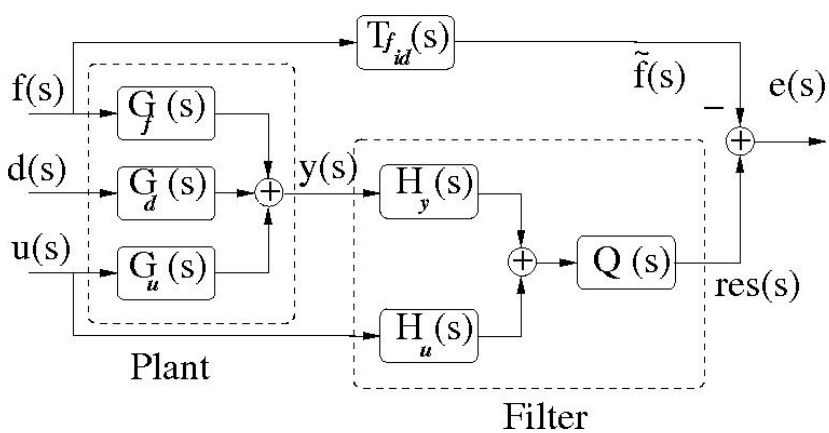

Figure IV-5 H_∞ ideal fault matching problem formulation

V. H-infinity FDI Filter Design and Gain Scheduling

Based on the stable LTI models of the Hopper RLV vehicle, here LTI FDI filters are designed at all the 19 trim points detailed in Section III using the model-matching H-infinity FDI design approach detailed in Section IV. A GS FDI filter is then designed based on the scheduling of three of these point-design filters over the considered reentry period of 90 seconds.

D. H-infinity FDI interconnection

The FDI design problem is posed as a standard $M-\Delta$ H-infinity control problem in LFT form, with the system interconnection depicted in Figure V-1. Here G_{si} is the nominal stable lateral LTI vehicle model presented in Section III and F is the FDI filter to be designed. The gain matrices K_a and K_s correspond to selector matrices, which determine the input and output channels affected by the actuator and sensor faults respectively (specifically the fifth actuator (rudder) and the third sensor (sideslip angle)). To capture the uncertainly that is inherent in the system and to provide for robustness to this uncertainty in the FDI filters, general input multiplicative uncertainty was also included in the system interconnection, as depicted by Δ_a in Figure V-1. The weighting matrices denoted by W_* correspond to those standard in H-infinity FDI design[6,3] and are employed to shape the FDI problem.

As in any H-infinity design, the choice of the weighting matrices is important. The logic for the choice of the weighting matrices in the present FDI problem is as follows: the ideal fault models W_{fs}, W_{fs} are chosen to be low pass with a bandwidth capturing the desired fault response time; the error weights W_{fs}, W_{fs} are chosen to be low pass and determine the frequency range where actuate FDI is desired; the noise weight W_n is chosen to be high pass to capture the frequency content of the noise; the input uncertainty weight W_a is chosen to be high pass, with an amplitude dependent on the level of robustness desired.

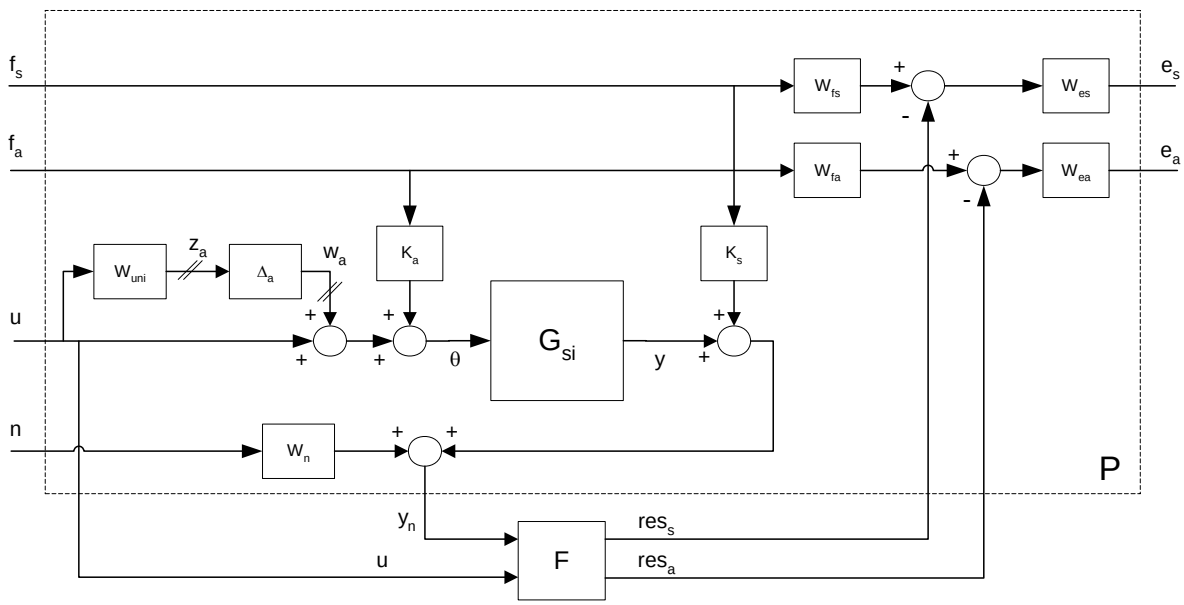

Figure V-1: H-infinity FDI Filter design interconnection.

With the LFT interconnection formed, a solution to the FDI problem can be found using H-infinity design theory[9]. This provides an FDI filter F that minimises the H-infinity norm of the system from the exogenous inputs of $M = F_l(P,F)$ to the error outputs of M, where M is the system formed via the lower LFT of F and P in Figure V-1. For the Hopper H-infinity FDI problem, M has the following input-output representation, where the partitioning of M separates the uncertainty inputs and outputs from the exogenous inputs and outputs:

$$\begin{bmatrix} z_a \\ \hline e_s \\ e_a \end{bmatrix} = \begin{bmatrix} M_{11} & M_{12} \\ M_{21} & M_{22} \end{bmatrix} \begin{bmatrix} w_a \\ \hline f_s \\ f_a \\ u \\ n \end{bmatrix}$$

Here w_a is the output of the actuator multiplicative uncertainties, f_s and f_a are the sensor and actuator faults, u is the commanded input, and n the sensor noise. The outputs are z_a, the input to the actuator multiplicative uncertainty, and e_s and e_a, the weighted error in the sensor and actuator fault estimation. Note that the filter F takes as inputs the output measurement with noise, y_n, and the commanded input u, and it outputs $\hat{f} = \begin{bmatrix} \hat{f}_s^T & \hat{f}_a^T \end{bmatrix}^T$, the fault estimate (equivalently res_s and res_a).

For the Hopper FDI problem depicted in Figure V-1, the submatrices of M are as follows

$$M_{11} = [0],$$

$$M_{12} = \begin{bmatrix} 0 & 0 & W_{uni} & 0 \end{bmatrix},$$

$$M_{21} = \begin{bmatrix} -W_{es} F_{sy} G_{si} \\ -W_{ea} F_{ay} G_{si} \end{bmatrix},$$

$$M_{22} = \begin{bmatrix} W_{es}\left(W_{fs} - F_{sy} K_s\right) & -W_{es} F_{sy} G_{si} K_a & -W_{es}\left(F_{su} + F_{sy} G_{si}\right) & -W_{es} F_{sy} W_n \\ -W_{ea} F_{ay} K_s & W_{ea}\left(W_{fa} - F_{ay} G_{si} K_a\right) & -W_{ea}\left(F_{au} + F_{ay} G_{si}\right) & -W_{ea} F_{ay} W_n \end{bmatrix},$$

where G_{si} is the nominal lateral Hopper model (stable), K_a and K_s are the selector matrices and the FDI filter F has the following partition, which corresponds to the inputs and outputs of the filter:

$$F = \begin{bmatrix} F_{sy} & F_{su} \\ F_{ay} & F_{au} \end{bmatrix}.$$

The equation for the weighted fault estimation error $e = \begin{bmatrix} e_s^T & e_a^T \end{bmatrix}^T$ is therefore given by

$$e_s = -W_{es} F_{sy} G_{si} w_a + W_{es}\left(W_{fs} - F_{sy} K_s\right) f_s - W_{es} F_{sy} G_{si} K_a f_a - W_{es}\left(F_{su} + F_{sy} G_{si}\right) u - W_{es} F_{sy} W_n n$$

$$e_a = -W_{ea} F_{ay} G_{si} w_a - W_{ea} F_{ay} K_s f_s + W_{ea}\left(W_{fa} - F_{ay} G_{si} K_a\right) f_a - W_{ea}\left(F_{au} + F_{ay} G_{si}\right) u - W_{ea} F_{ay} W_n n$$

E. Design of LTI H-Infinity FDI Filters

With the FDI problem now represented in the standard LFT representation, LTI FDI filters can be designed using H-infinity design tools, with the Matlab *hinfsyn* algorithm employed[9]. This synthesises LTI FDI filters having 11 inputs (6 plant outputs and 5 control inputs) and two outputs (fault estimates for the sensor fault and actuator fault). Each filter is comprised of 20 states. Based on the system interconnection and the choice of the fault selectors K_a and K_s, each LTI FDI filter is designed to *simultaneously* detect and isolate faults in the rudder actuator and sideslip sensor, and to decouple commands in all input channels. They are also designed to do this robustly, based on the general input multiplicative uncertainty model used in the H-infinity design, as shown in Figure V-1.

Figure V-2 below shows the Bode magnitude plot of the designed point FDI filters for all the 19 trim points detailed in Section III. From the figure it is clear that the qualitative shape of all the FDI filters is very similar. This is to be

expected, as very similar design weights were used for all the H-infinity FDI point designs and the LTI plants at each trim point have the same qualitative features. It is however clear that the low frequency gains of the filters vary significantly due to significant variation in the low frequency gains of the plant models over the re-entry period. Hence one would expect robustness to be poor at low frequencies for certain inputs, and that a single LTI FDI filter is unlikely to work well over the full 90 second re-entry period considered. Conversely, some elements of the FDI filter are essentially identical for all the point-design filters and hence the corresponding response of the point-design FDI filters will be robust to the plant variation over the re-entry period (These features are confirmed in the simulations presented in Section VI).

F. Design of a Gain-Scheduled H-Infinity FDI Filter

Once the LTI filters were obtained, it was observed (see Section VI and Figure VI-2), that the point-design FDI filters had limited performance/robustness properties when applied at trim points away from that for which they were designed and hence also to the GS plant. This is particularly the case for FDI of actuator faults. Thus, it was decided to perform a scheduling of a subset of the point-design LTI FDI filters to evaluate the gain scheduling capabilities of the FDI controllers and improve the filter robustness to parameter variations.

Three point-design LTI FDI filters were chosen for scheduling over the 90 second period, being those at trim times 1420, 1451 and 1480. These trim times were chosen to cover uniformly the re-entry period. Based on past experience with this type of vehicle, a quadratic scheduling law based on time was chosen (It is noted that time is linearly related to velocity in this flight region, see Figure II-1, so more practical velocity scheduling can easily be obtained).

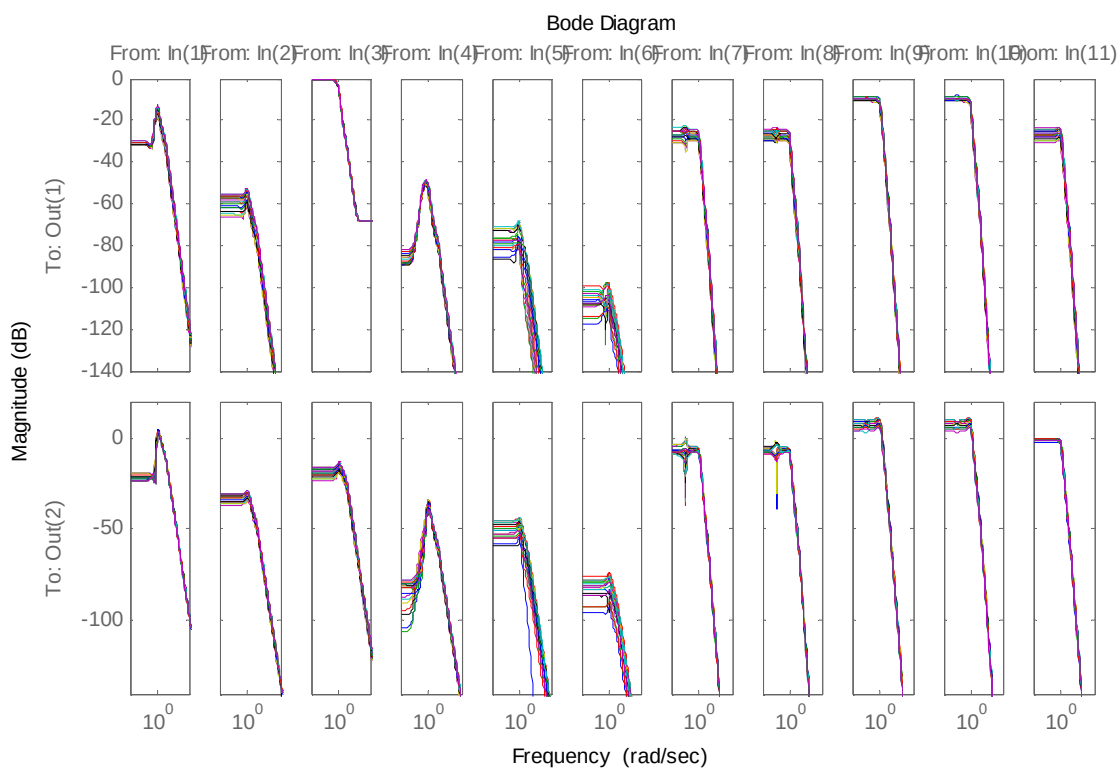

Figure V-2: Bode magnitude plot of all 19 point-design FDI filters.

VI. Open-loop FDI Filter Evaluation

In this section the fault estimation capabilities of a selection of the designed LTI FDI filters and the GS filter are shown for faults corresponding to the fault scenario described in Section II. This is done with the plant model for the re-entry period *frozen* at one of the LTI plant models and also for a *GS plant* that is formed by interpolating between *all 19 LTI models* covering the reentry period. The response of this latter GS plant best approximates the time varying vehicle dynamics over this reentry period. More specifically, the time responses of the point-design LTI

filters designed at times 1420 and 1480 (F_1420 and F_1480) and the GS filter, are evaluated in open-loop using the corresponding LTI plants (stable plants) at times 1420 and 1480 (P_1420 and P_1480) and the GS plant.

The time responses are shown in two sections. The first section shows time responses designed to highlight the features of the LTI and GS FDI filters when applied to the frozen LTI plant models and the more realistic GS plant. The second section presents a more exhaustive comparison of these features. It should be emphasised that in the simulations, the GS plant is scheduled based on models at every 5 seconds (approximately) in the trajectory using standard linear interpolation algorithms while the GS filter is only scheduled based on three point-design FDI filters (F_1420, F_1451 and F_1480) and quadratically scheduled. In addition, the GS filter scheduling is delayed by 1 second. Hence this assessment provides a measure of the performance of an LTI FDI filter at its design point (ie on the LTI plant for which is was designed), its robustness with respect to a different LTI plant and its behaviour in the face of a dynamically changing, and more realistic, GS plant. Similarly, it will allow examination of the equivalent characteristics for the GS filter.

In all the response plots presented in the proceeding sections, the sensor (sideslip angle) fault signals and actuator (rudder) fault signals are applied *simultaneously* to the vehicle in the same sequence of steps and ramps. Figure VI-1 shows the input commands used in those cases that considered them. The commands correspond to repeated sets of low and high frequency signals and are applied in a manner that would produce both lateral/directional motion and longitudinal motion. However, due to the removal of the longitudinal attitude states in the model, the effect on the this motion is negligible (These inputs were tested on the full stable LTI vehicle model and the inclusion of the longitudinal states had negligible effect on the lateral vehicle response, due to the strong lateral-longitudinal response decoupling in the vehicle, and hence no effect on the fault estimates). Note that the control inputs are quite aggressive, with inputs of up to 5 degrees in the elevons and 6 degrees in the rudder. As perturbations from trim levels, which these signals represent, these correspond to the upper range of that seen in the closed-loop system[1].

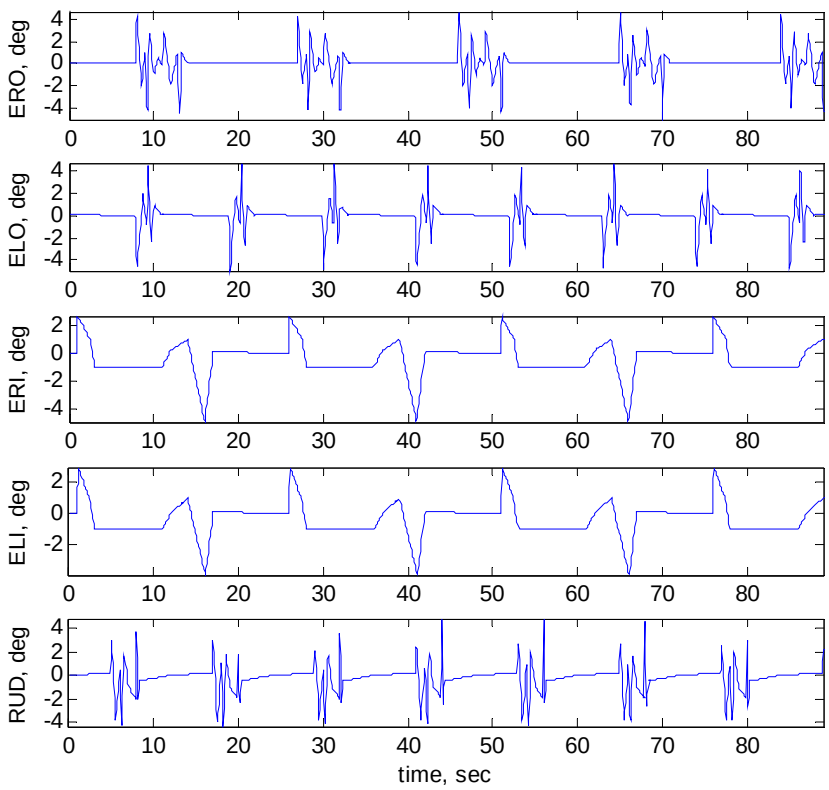

Figure VI-1: Commands used in open-loop simulations (degrees)

In addition to fault and actuator commands, realistic levels of sensor noise are added to the plant outputs. The noise levels are based on those in Ref.1 and are generated by independent random number generators in each channel. For the output channels (roll rate p, yaw rate r, sideslip beta, bank angle sigma, velocity Vt and geocentric altitude R) the noise signals are uniformly distributed signals, centered at zero with maximum amplitude being {0.01,0.01,0.1,0.1,1,10} degrees, respectively.

Remark: Note that in the response plots to follow, the GS plant and filter are continuously scheduled. Hence the GS plant is approximately that for the LTI plant at the trim point corresponding to the trim point times. It is for this reason that one sees the LTI FDI filters performing well when applied to the GS plant around the simulation time corresponding to their point design. Similarly, when the GS filter is applied to a fixed LTI plant (P_1420 or P_1480) over the full time period, one sees that is works best for this plant around the response time corresponding to the LTI plant, as it is here that the GS filter best approximates the point-design filter for that trim time. *Note that all shown simulation times are relative to the reentry time of 1410 seconds.*

G. Exemplary Simulations

4. Point-design Filter

Here a representative figure for the point-design FDI filter responses is shown to highlight the properties of the LTI filters. Figure VI-2 shows the response of the filter designed at trim point 1420 (F_1420) when applied to the FDI problem for the LTI plant at 1420. The response is also shown for the LTI plant at 1480 and for the GS plant. All plots are shown for the full time period (ie 1410 to 1500 seconds). It should be noted that for the LTI plant responses, the simulation corresponds to the response of the point-design FDI filter F_1420 considering this LTI plant for the whole period. Conversely, for the GS plant response, the plant is continuous updated (scheduled) to capture the linearised response of the vehicle at each of the trim points corresponding to the simulation time (ie each 5 seconds).

From Figure VI-2 it is seen that the point-design FDI filters perform well at their designed trim point, as would be expected, but at other trim points, and similarly for the GS plant for this re-entry period, the performance can be significantly worse. This is particularly the case for the actuator fault FDI, while it is seen that the sensor fault FDI properties are quite robust.

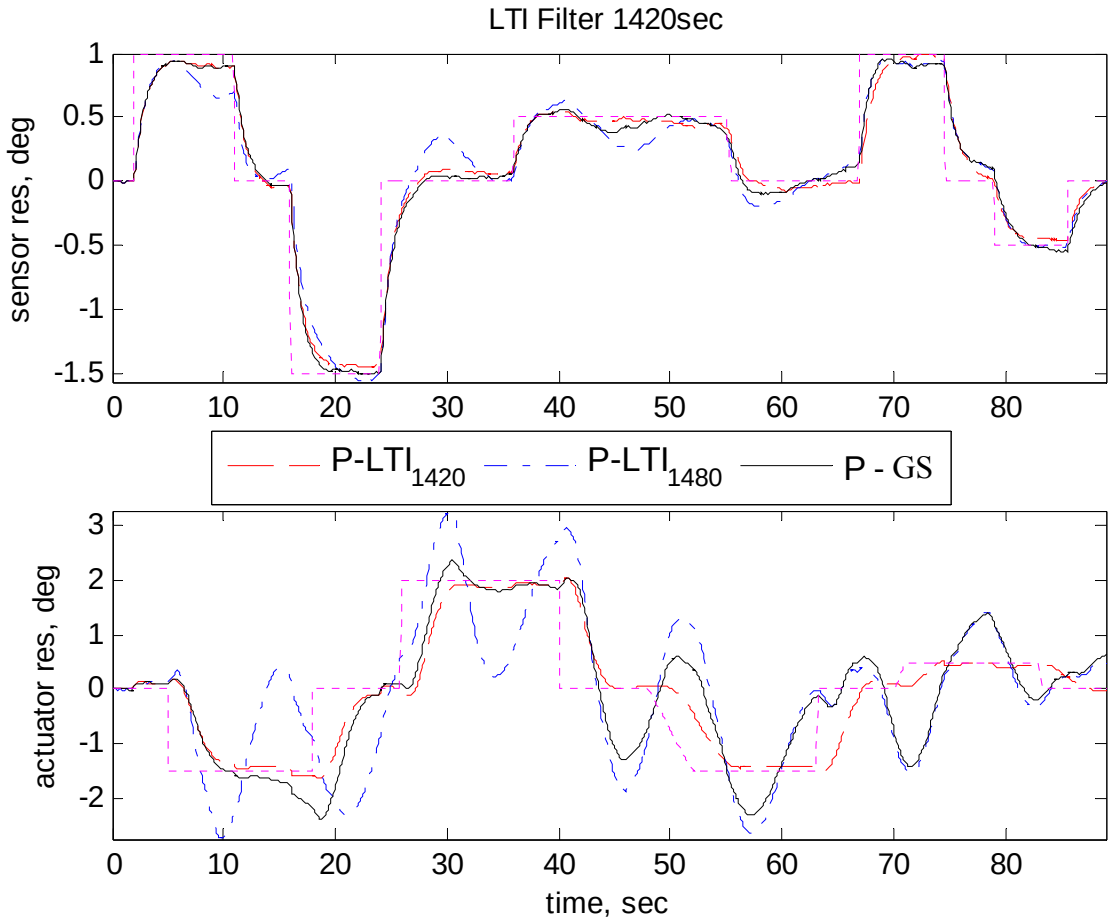

Figure VI-2: Filter F_1420 applied to LTI plants P_1420 and P_1480, and GS plant P_GS (fault estimate in degrees)

5. Gain-Scheduled Filter

Here a representative figure for the GS filter response is shown to highlight the properties of the GS filter. Figure VI-3 shows the response of the GS filter when applied to the FDI problem for the GS plant for the full time period (ie 1410 to 1500 seconds) and also the LTI plants at 1420 and 1480 seconds. The actuator commands for the system are shown in Figure VI-1. The simulations show that the GS filter performs about as well as the point-design FDI filters at their corresponding trim points, and quite well between the trim points used for the scheduling, and hence overall has a superior FDI response to that of the point-design LTI FDI filters when applied to the realistic GS plant for the reentry period. Consequently, as the GS plant is most representative of the vehicle response over the re-entry period considered, it is evident that the GS filter is superior. This is particularly the case for the actuator fault FDI, while for sensor fault FDI the GS filter performs only slightly better than that for the points designs when applied to the GS plant. In particular, the control decoupling is better for the GS filter.

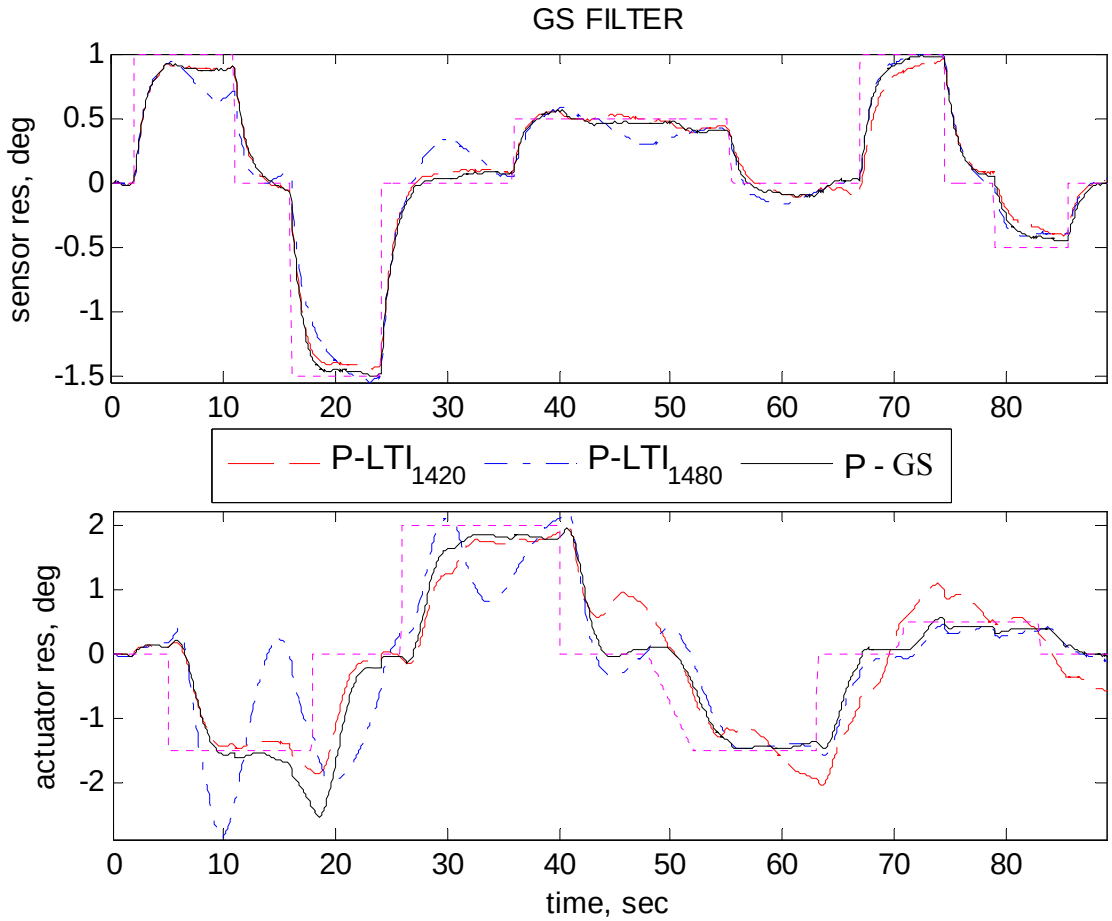

Figure VI-3: GS filter applied to LTI plants P_1420 and P_1480, and GS plant P_GS (fault estimate in degrees)

H. Additional Simulation Cases

To support the findings in the previous selection, over the proceeding pages the results for the 4 simulation cases specified in Table VI-1 are presented and discussed. (Note that the noise and control signals are as detailed previously, with noise always present in the simulations).

Table VI-1 Open-loop simulation cases

CASE	COMMANDS	SENSOR FAULT	ACTUATOR FAULT
1	YES	NO	NO
2	YES	BETA	NO
3	YES	NO	RUD
4	YES	BETA	RUD

For each case/figure six plots are given: the three plots in the top row show the sensor fault estimation responses, while the bottom row shows the actuator fault estimation responses. The first column shows the response of the point-design LTI filter designed at time 1420, the second column that of the point-design LTI filter designed at time 1480 and the last column the GS filter. Within each individual plot there are four lines: dotted-magenta for the fault, dashed-red for the responses using the LTI plant at 1420, dashed-dot-blue for those using the LTI plant at 1480 and the solid-black for those using the GS plant (the more realistic plant).

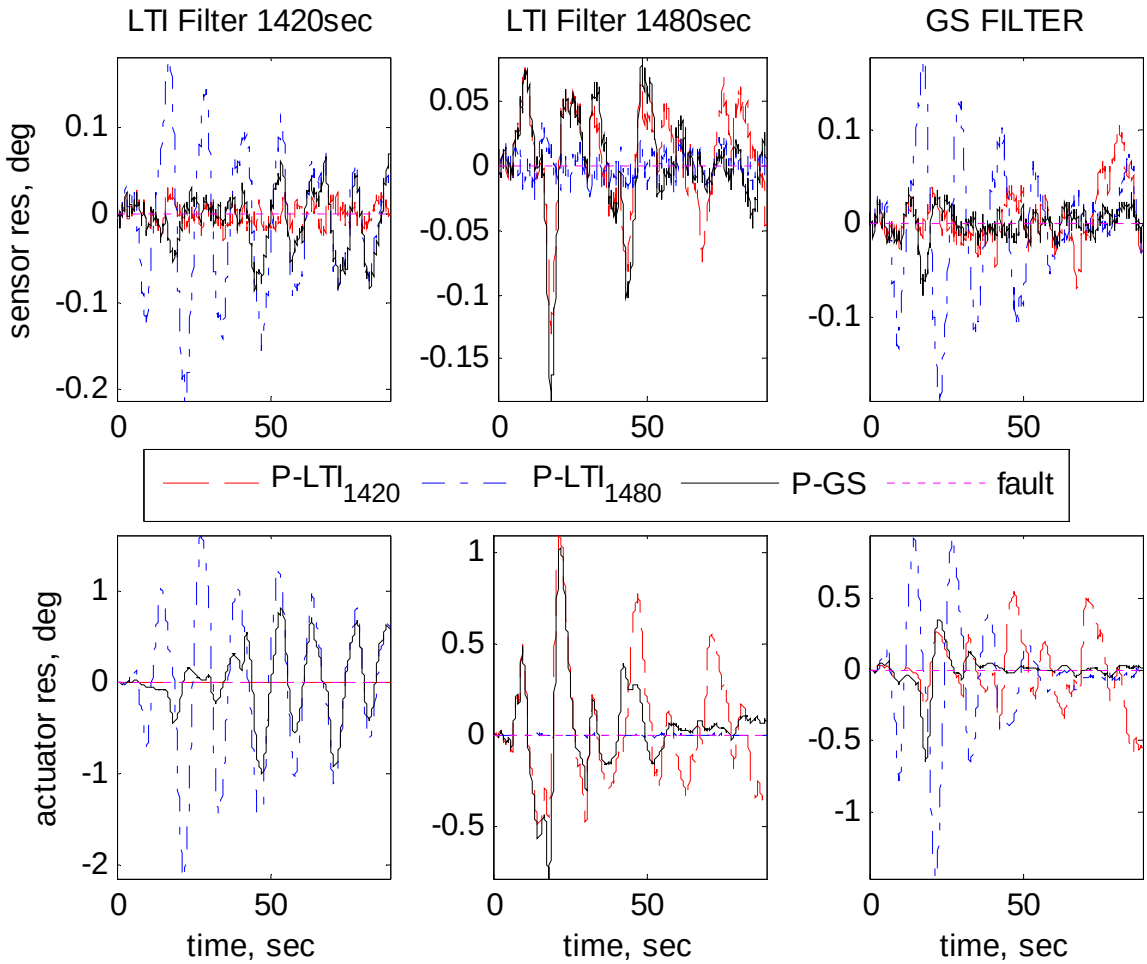

Figure VI-4 CASE 1: only commands and noise (fault estimate in degrees)

I. Summary of Results

Based on the simulation results, one can conclude that:

i. The sensor residual is the most robust and has the best FDI characteristics, with only minor coupling due to commands.

ii. The actuator residual suffers from some coupling from the sensor fault and is not very robust to changes in plant, as demonstrated by the point-design filters. It also contains a non-minimum phase (NMP) response behaviour that slows the detection time but is otherwise acceptable.

iii. The LTI filters are properly designed for their LTI plant counterparts but are not very robust to changes in the vehicle behaviour. This was expected, given the challenging synthesis problem arising from the numerous input/output channels and significant level of variation in the plant dynamics arising from the vehicle tracking the re-entry trajectory.

iv. The main lack of robustness of the LTI filters arises from the command and sensor fault coupling on the actuator fault estimate. As seen in the figures, a GS filter formed from three of the point-design LTI filters suffices to improve this lack of robustness to an acceptable level.

v. The GS filter shows a superior performance, with the FDI capabilities always at least as good as the LTI FDI filters when simulated at their design points[§§]. The improvement from its employment is clearly seen for the case of actuator faults, with the improvement of the sensor fault estimate only minor (in control decoupling). The inherent robustness of the sensor fault estimate is not surprising, given that sensor fault effects are typically less sensitivity to plant uncertainty/variation.

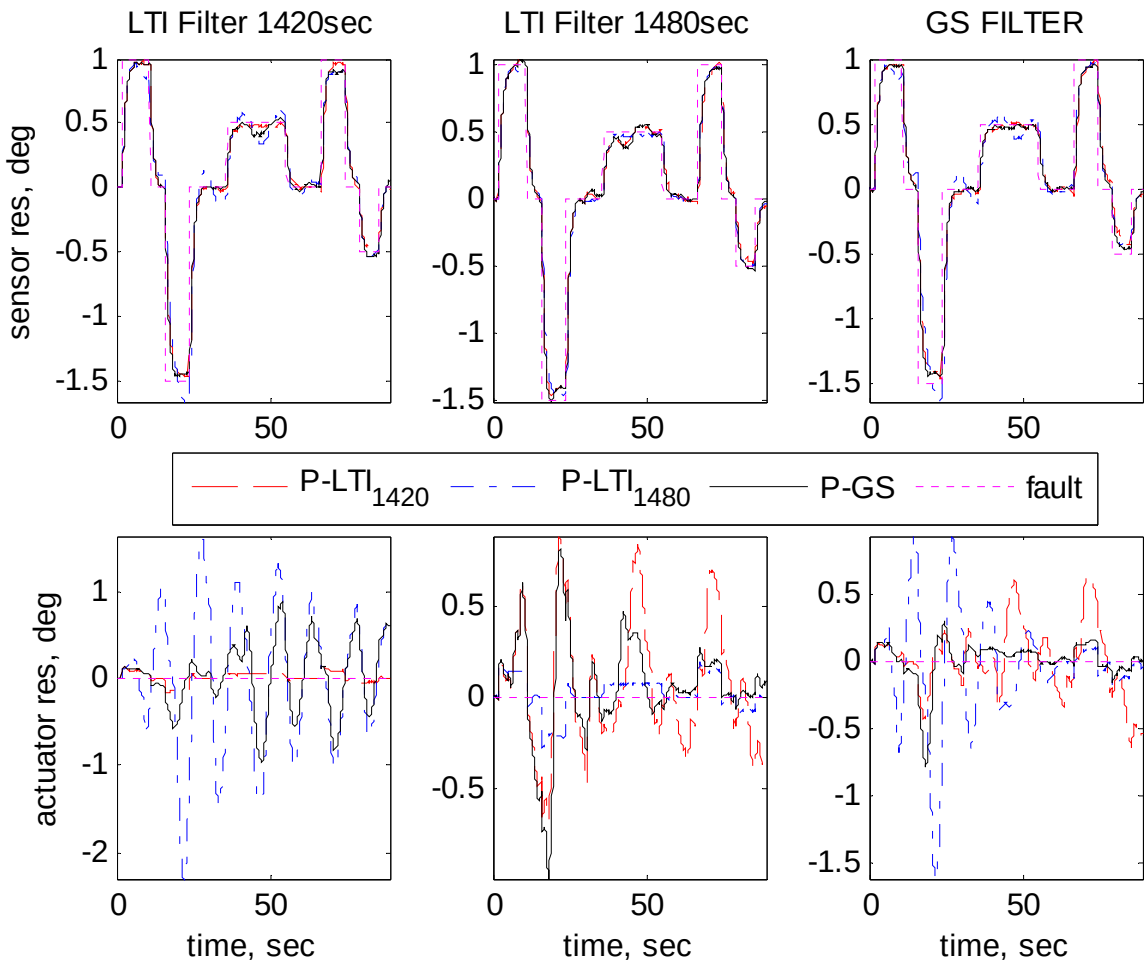

Figure VI-5 CASE 2: sensor fault, commands and noise (fault estimate in degrees)

[§§] Recall that the GS filter scheduling is delayed by 1 second and is therefore not the same filter as the point-design FDI filters used in the scheduling at their design point.

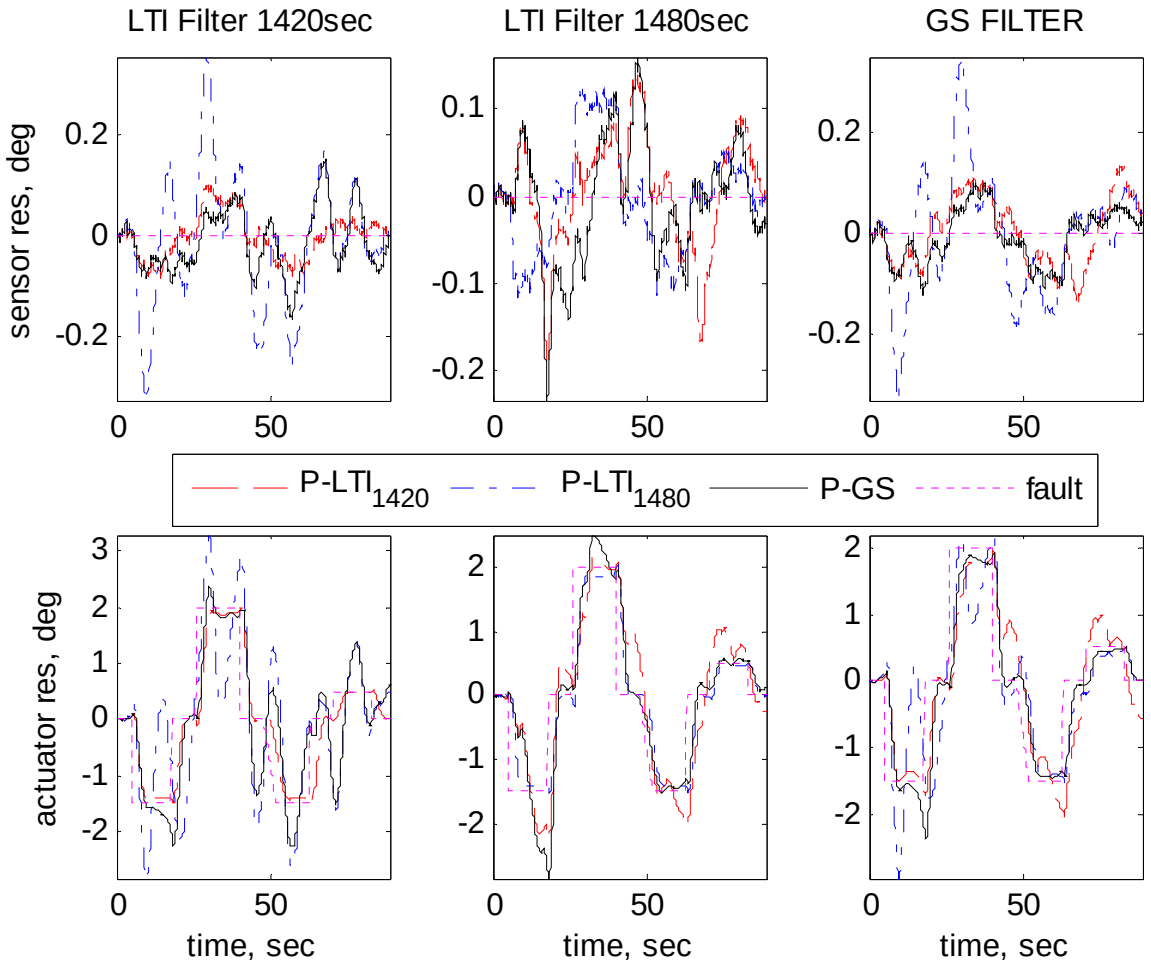

Figure VI-6 CASE 3: actuator fault, commands and noise (fault estimate in degrees)

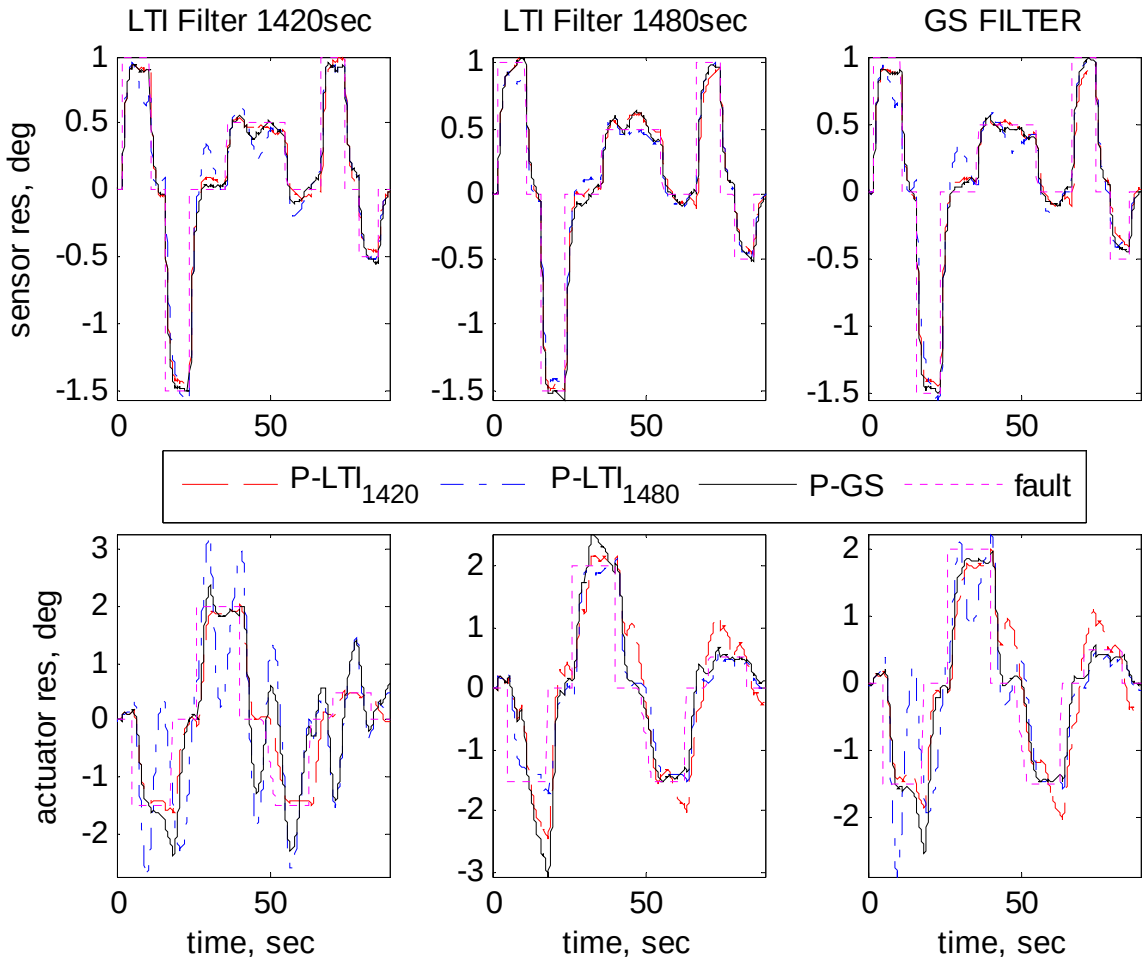

Figure VI-7 CASE 4: sensor and actuator fault, commands and noise (fault estimate in degrees)

VII. Conclusions & Future Work

This paper presented the design and open-loop evaluation of point-design LTI and gain-scheduled open-loop FDI filters for the Hopper RLV. The filters were designed to provide for FDI on stable LTI models of the Hopper vehicle, with the filters designed based on H-infinity theory. The FDI scenario considered was found to be challenging due to the variation of the vehicle dynamics as it tracks the re-entry trajectory, the subsequent high level of effective plant uncertainty for each of the point-design FDI filters, the high number of control inputs and the choice of simultaneous FDI for two faults that inherently couple (rudder actuator and sideslip sensor). The effectiveness of the filters for FDI was evaluated via their application to frozen LTI models of the vehicle and also to a more realistic gain-scheduled model of the vehicle over the considered 90-second re-entry period. It was shown that the point-design FDI filters had limited performance/robustness properties when applied at trim points away from that for which they were designed and hence were incapable of providing for adequate FDI capabilities over the full re-entry period. Gain scheduling these filters was seen to overcome this lack of robustness and provide for good FDI over the full period. It is therefore evident that for re-entry vehicles, parameter varying FDI filters are necessary for the provision of adequate FDI performance.

Recently the FDI design process presented here for the stable LTI Hopper model has been extended and employed for the design of open-loop FDI filters on the unstable and nonlinear Hopper vehicle. This problem considered

similar fault scenarios to that considered herein, being faults on the rudder actuator and sideslip sensor. Figure VII-1 shows the fault estimates provided by the designed FDI filter over the same 90 second period for the nonlinear and unstable Hopper RLV in closed-loop with the NDI controller in Ref.1. The figure shows the response for 100 (out of 1000) cases from a Monte-Carlo campaign. The uncertainty levels considered are consistent with those detailed in Ref.1. The faults are steps of 0.3 degrees and 2 degrees in the beta sensor and rudder actuator, respectively, which are active for 20 seconds and then slowly decrease back to zero.

These preliminary results show that for the sensor fault case the designed FDI filter has provided for robust and accurate FDI, with only a small error in the identified fault signal. There is however significant coupling to the actuator fault estimate, as expected, given that the beta sensor and rudder actuator faults have similar effects on the vehicle's lateral response. For the actuator fault case the results show that the designed FDI filter also provides for robust and accurate fault detection and isolation, with significant but smaller coupling to the sensor fault estimate.

These preliminary results on FDI for the unstable and nonlinear vehicle agree with the results presented in Section VI, in that again actuator FDI is found to be more difficult, as seen here with larger coupling to the actuator fault estimate from the sensor fault. Continuing work is focusing on the improvement of the robustness of these results and the use of post filtering logic to provide fault detection and isolation capabilities suitable for use in a health management system (HMS) or for fault tolerant control (FTC). The outcomes from the completion of this work will be reported shortly.

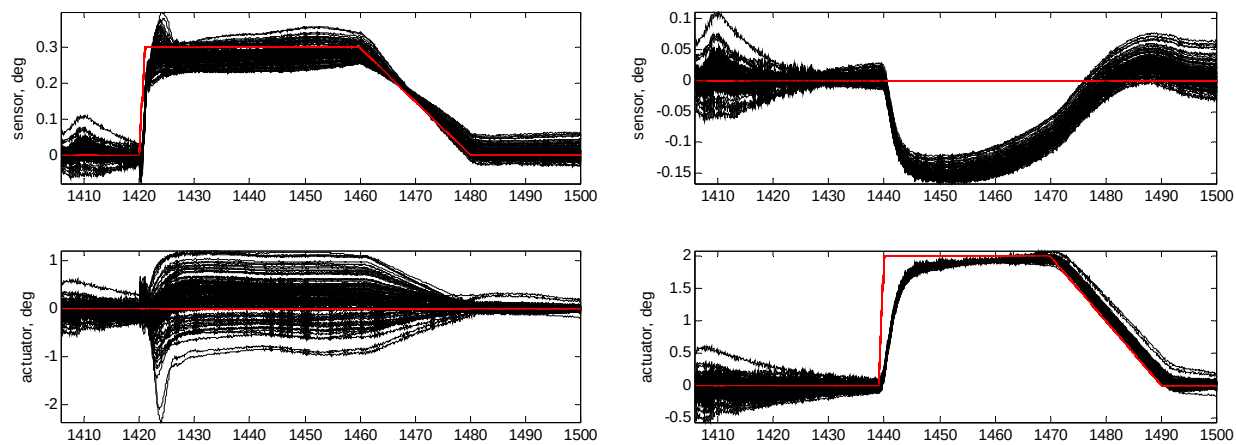

Figure VII-1 Fault estimates for 100 out of 1000 runs from a Monte-Carlo Campaign: Beta sensor fault of 0.3 degree maximum amplitude and fault estimates; Rudder actuator fault of 2 degree maximum amplitude and fault estimates.

Acknowledgments

This worked was performed within the ESA project "Health Management for Reusable-space Transportation". The authors would like to thank EADS Astrium, the leaders of this project, who provided the model of the Hopper RLV used in the present work.

References

[1] Marcos, A., Peñín, L.F., Caramagno, A., Sommer, J., Belau, W., "Atmospheric Re-Entry NDI Control Design for the Hopper RLV Concept," *Proceedings of the 17th IFAC Symposium on Automatic Control in Aerospace*, Toulouse, July 2007.

[2] Augustin, R.M., Mangoubi, R.S., Hain, R.M., Adams, N.J., "Robust failure detection for reentry vehicle attitude control systems," *Journal of Guidance, Control, and Dynamics*, Vol. 22, No. 6, 1999.

[3] Castro H., Bennani S., Marcos A. "Robust filter design for a Re-entry Vehicle," *Proceedings of the 7th International Conference on Dynamic and Control of Systems and Structures in Space*, UK, July, 2006.

[4] Marcos, A., De Zaiacomo, G., Peñín, L.F., Bornschlegl, E., "Fault Analysis for Robust FDI Design During RLV Ascent and Re-entry Phases," 7th International ESA Conference on Guidance, Navigation and Control Systems. Tralee, Ireland, June2008.

[5] Seron, M.M.; Goodwin, G.C., "Design limitations in linear filtering", Proceedings of the IEEE Conference on Decision and Control, 1995, pp. 1519 - 1524.

[6] Chen, J., Patton, R.J., *Robust Model-based Fault Diagnosis for Dynamic Systems*, Kluwer Academic Publishers: Dordrecht, 1999.

[7] Niemann H., Stoustrup J. "Robust Fault Detection in Open Loop vs. Closed Loop," *Proceedings of the 36th IEEE Conference on Decision and Control*, 1997, pp. 4496-4497.

[8]Marcos, A., *Aircraft Application of Fault Detection and Isolation Techniques*, PhD. Thesis, University of Minnesota, USA, February 2004.

[9] Balas, G.J., Doyle, J.C., Glover, K., Packard, A., Smith, R., *mu-Analysis and Synthesis Toolbox*, The Mathworks & MUSYN INC.

[10] Skogestad, S., Postlethwaite I., *Multivariable Feedback Control - Analysis and design*, Wiley, 1996.